Published in final edited form as:
J Neurochem. 2010 November ; 115(4): 984–993. doi:10.1111/j.1471-4159.2010.06990.x.

Search for the acetylcholine and vesamicol binding sites in vesicular acetylcholine transporter: the region around the lumenal end of the transport channel

Parul Khare, **Anuprao Mulakaluri**, and **Stanley M. Parsons***
Department of Chemistry and Biochemistry, Neuroscience Research Institute, University of California, Santa Barbara 93106

Abstract

Vesicular acetylcholine transporter (VAChT; TC 2.A.1.2.13) mediates storage of acetylcholine (ACh) by synaptic vesicles. A three-dimensional homology model of VAChT is available, but the binding sites for ACh and the allosteric inhibitor vesamicol are unknown. In previous work, mutations of invariant W331 in the lumenal beginning of transmembrane helix VIII (TM VIII) of rat VAChT led to as much as 9-fold loss in equilibrium affinity for ACh and no loss in affinity for vesamicol. The current work investigates the effects of additional mutations in and around W331 and the nearby lumenal end of the substrate transport channel. Mutants of human VAChT were expressed in the $PC12^{A123.7}$ cell line and characterized using radiolabeled ligands and filtration assays for binding and transport. Properties of a new and a repeat mutation in W331 are consistent with the original observations. Of sixteen additional mutations in thirteen other residues (Y60 in the beginning of lumenal Loop I/II, F231 in the lumenal end of TM V, W315, M316, K317, in the lumenal end of TM VII, M320, A321, W325, A330 in lumenal Loop VII/VIII, A334 in the lumenal beginning of TM VIII, and C388, C391, F392 in the lumenal beginning of TM X), only A334F impairs binding. This mutation decreases ACh and vesamicol equilibrium binding affinities by 14- and 4-fold, respectively. The current results, combined with previous results, demonstrate existence of a spatial cluster of residues close to vesicular lumen that decreases affinity for ACh and/or vesamicol when the cluster is mutated. The cluster is composed of invariant W331, highly conserved A334, and invariant F335 in TM VIII and invariant C391 in TM X. Different models for the locations of the ACh and vesamicol binding sites relative to this cluster are discussed.

Keywords

vesicular acetylcholine transporter; acetylcholine; transporter; synaptic vesicle; vesamicol

Vesicular acetylcholine transporter (VAChT; TC 2.A.1.2.13)[1] is an integral membrane protein found in synaptic vesicles of cholinergic nerve terminals (Parsons 2000). It mediates filling of vesicles with the neurotransmitter acetylcholine (ACh) in preparation for evoked release of ACh from nerve terminals. Transport is driven by exchange of vesicular protons for

*To whom correspondence should be addressed: Department of Chemistry and Biochemistry, University of California, Santa Barbara, CA 93106-9510. parsons@chem.ucsb.edu. Telephone: (805) 893-2252. Fax: (805) 893-4120.

[1]Abbreviations: ACh, acetylcholine; B_{max}, maximal binding of [^{3}H]vesamicol; F_{HA}, fraction of ACh binding sites that exhibit high affinity at equilibrium; glycerol-3-phosphate phosphate antiporter, GlpT; hVAChT, human VAChT; K_V, equilibrium dissociation constant for vesamicol binding; K_{AChHA}, equilibrium dissociation constant for binding of ACh to its high-affinity site; K_{AChLA}, equilibrium dissociation constant for binding of ACh to its low-affinity site; K_M, Michaelis-Menten constant for transport of [^{3}H]ACh; MFS, major facilitator superfamily; rVAChT, rat VAChT; TM, transmembrane helix; UBB, uptake binding buffer, VAChT, vesicular acetylcholine transporter; vesamicol, ( )-*trans*-2-(4-phenylpiperidino)cyclohexanol; V_{max}, maximal velocity for transport of [^{3}H]ACh.

cytoplasmic ACh. A synthetic compound called vesamicol binds to and inhibits VAChT (Bahr *et al.* 1992). The locations of the ACh and vesamicol binding sites are unknown.

VAChT is a member of the major facilitator superfamily (MFS) (Saier *et al.* 1999). A three-dimensional model of VAChT has been constructed by Schuldiner and colleagues (Fig. 1) based on the crystal structure of the MFS protein glycerol-3-phosphate phosphate antiporter (GlpT) and sequence homology (Vardy *et al.* 2004). Transmembrane helices I–VI (TMs I–VI) are packed into one bundle and the remaining TMs VII–XII are packed into another bundle. The bundles contact each other with convex surfaces and create a central transport channel approximately perpendicular to the plane of the membrane. The mouth of the channel that would be inside a synaptic vesicle is closed, and the mouth that would be in cytoplasm is open. Rocking of the bundles against each other is hypothesized to expose a single substrate binding site in the channel alternately to one side of the membrane and then to the other (Abramson *et al.* 2004; Law *et al.* 2008b). The motion is called “rocker switch.”

In many documented cases, the substrate binding site lies approximately midway through the transport channel and in the center of the membrane (Yang *et al.* 2005; Law *et al.* 2008a; Patching *et al.* 2008; Jeon *et al.* 2009; Law *et al.* 2009; Eudes *et al.* 2010). However, bound substrates make contacts with different TMs. The lack of a universal binding site means that the location for ACh binding to VAChT cannot be deduced from information available from other MFS transporters. Moreover, some evidence suggests the rocker-switch model of transport with its single binding site for substrate may not apply to all members of the MFS (Adler and Bibi 2004; Tsigelny *et al.* 2008; Carruthers *et al*. 2009).

In a prior search for the ACh binding site, mutations of W331 in rat VAChT (rVAChT) were found to decrease ACh affinity up to 9-fold without affecting vesamicol affinity, thereby demonstrating that mutation of W331 perturbs the structure of VAChT to a limited extent. Accordingly, W331 was hypothesized to be in the ACh binding site (Ojeda *et al.* 2004). Residue numbers used in the current manuscript apply to both human VAChT (hVAChT) and rVAChT. Residues invariant in 12 phylogenetically diverse species are shown in boldface font from here forth. A “highly conserved” residue occurs in >70% of VAChTs.

The VAChT homology model locates **W331** in the closed section of the transport channel close to vesicular lumen. To bind next to **W331**, ACh would have to diffuse from cytoplasm through the open part of the channel, which is filled with water, and through a portion of the closed part of the channel near vesicular lumen. The latter step probably is possible, as analysis of the homology model with the program “Computed Atlas of Surface Topography of Proteins” (CASTp) reveals several pockets and cavities in the vicinity of **W331** caused by loose side-chain packing (Dundas *et al.* 2006).

Three additional considerations support this possibility. First, the VAChT homology model is of uncertain accuracy. It almost surely is approximately correct, but probably not to high resolution. Second, the precedent for binding substrate to a single site approximately midway through the channel is limited, as relatively few such sites in MFS proteins have been definitively located. Third, the type of physiological role that VAChT has is atypical. VAChT must release newly transported ACh into the lumen of synaptic vesicles containing concentrated ACh in order to complete the filling process (Volknandt and Zimmermann 1987). Net release requires the dissociation constant to be >100 mM. Severe disruption of the ACh site might be required to make the dissociation constant that large. Such disruption possibly can be accomplished best by locating the ACh binding site in the closed part of the channel so the site is torn asunder when VAChT rocks to face vesicular lumen.

The kinetics of inhibition by vesamicol, structure-function analyses of ACh and vesamicol analogues, and the properties of VAChT mutants have demonstrated that the ACh and

vesamicol binding sites are at least partially distinguishable from each other (Rogers and Parsons 1989; Bahr *et al.* 1992; Kim *et al.* 1999). However, no clear picture of their locations has emerged. The binding site for ACh clearly is of intrinsic interest. More extensive testing of whether it is next to **W331** is needed. The binding site for vesamicol also is of interest, as analogues incorporating imaging isotopes like positron-emitting ^{18}F are being developed for clinical diagnostics (Tu *et al.* 2009). It might be possible to design better analogues if the location of the vesamicol binding site were known. The current report reveals the properties of mutants in and around **W331** and the closed portion of the transport channel.

Materials and methods

Cell culture

PC12$^{A123.7}$ cells were grown at 37 °C in an atmosphere of 10% CO_2 in complete Dulbecco's modified Eagle's medium mixed 1:1 with Ham's F-12 medium. The medium was supplemented with 10% horse serum, 5% fetal bovine serum, 100 units penicillin/mL, 100 μg streptomycin/mL, and 10 μg blasticidin/ml (complete medium).

Site-directed mutagenesis and stable transfection

The cDNA for hVAChT was obtained from Invitrogen and transferred into pcDNA 6.2/V5-destination vector using the LR Recombinase method (Invitrogen). Mutations in hVAChT were made using the Stratagene QuikChange kit according to the manufacturer's instructions. Primers for mutagenesis were obtained commercially. Plasmids were purified from XL1-Blue Supercompetent cells (Stratagene) using a commercial kit (Qiagen). Mutated plasmids were sequenced by a commercial facility to ensure that the mutation was present. Purified plasmids were transfected into PC12$^{A123.7}$ cells with Lipofectamine in antibiotic-free complete medium. Blastcidin (10 μg/ml) was added to each plate to select for stable transfectants, which required 2–3 weeks of selection (Khare *et al.* 2009).

Western blot analysis and selection of stable clones

Western blot analysis of VAChT expressed by at least 12 clonal lines was performed for each mutant using standard technique. The most highly expressing clone was selected for growth in complete medium until sixteen 175 cm^2 flasks were confluent.

Preparation of post-nuclear supernatant

Cells were harvested, resuspended in 1 mL of 0.32 M sucrose, 10 mM N-(2-hydroxyethyl) piperazine-N'-2-ethanesulfonic acid (HEPES), 1 mM dithiothreitol, adjusted to pH 7.4 with KOH, fresh 100 μM phenylmethanesulfonyl fluoride (Sigma, St. Louis, MO), 100 μM diethyl *p*-nitrophenyl phosphate (paraoxon) and complete protease inhibitor cocktail (Roche, Mannheim, Germany) [homogenization buffer (HB)], and gently homogenized. The suspension was centrifuged at 1500*g* for 10 min, and postnuclear supernatant (10 – 15 mg protein/mL) was stored at −80 °C until used.

[^{3}H]Vesamicol saturation curves, ACh binding, and [^{3}H]ACh transport at pH 7.4

The detailed procedures for these assays have been described (Varoqui and Erickson 1996) and were used with minor modifications (Ojeda *et al.* 2004; Bravo *et al.* 2005b). In brief, for total binding (the sum of specific and non-specific binding) of [^{3}H]vesamicol, 20 μg of postnuclear supernatant was mixed with the volume of HB required to sum to 50 μL. This suspension was mixed with 100 μL 110 mM potassium tartrate, 20 mM HEPES (pH 7.4 with KOH), 1 mM dithiothreitol [uptake binding buffer (UBB)] and 50 μL of UBB containing four times the final concentration of [^{3}H]vesamicol. For total binding of [^{3}H]vesamicol in the presence of competing ACh, 20 μg of postnuclear supernatant in a total of 50 μL HB was mixed

with 100 μL of UBB containing 100 μM paraoxon and twice the final concentration of unlabeled ACh. After 10 min, the suspension was mixed with 50 μL of UBB containing 100 μM paraoxon and 20 nM [^{3}H]vesamicol. For total transport of [^{3}H]ACh, 250 μg of postnuclear supernatant in a total of 50μL HB containing 100 μM paraoxon was mixed with 50 μL of UBB containing 100 μM paraoxon. Transport was initiated by the addition of 100 μL of UBB containing 100 μM paraoxon, 12 mM MgATP, 10 mM $MgCl_2$, pH 7.4 with KOH, and twice the final concentration of [^{3}H]ACh. Suspensions were incubated for 10 min (or 5 min for transport) at 37 °C, and incubation was terminated by filtration (or quench-dilution and filtration for transport) and washing.

Filtration, washing and determination of bound radioactivity

Two 85 μL portions of each incubation were filtered rapidly through glass-microfiber circles (GF/F 1.3 cm diameter, Whatman) coated with 0.25% (w/v) poly(ethylenimine). The filters were quickly washed with four 1-mL portions of UBB containing 5 μM of (±)-vesamicol. [^{3}H]ACh was solubilized in 0.1% sodium dodecylsulfate. Radioactivity was determined by liquid scintillation spectrometry to an uncertainty of ≤ 3 % cpm or ≤ 10 min acquisition time. Non-specific binding or transport was determined in the presence of 80 μM of (±)-vesamicol during incubation.

Data analysis

Results of duplicates were averaged. Regression was performed by simultaneously fitting appropriate equations to total and nonspecific binding or transport with the software Scientist (Micromath Research, St. Loius, MO) as described (Bravo *et al.* 2005b). K_v is the half-saturation concentration and B_{max} is the maximal specific binding by [^{3}H]vesamicol per mg of post-nuclear supernatant. K_M and V_{max} are the usual Michaelis-Menten parameters for specific transport. Equilibrium binding of ACh to wild-type VAChT is biphasic due to high- and low-affinities (Bravo *et al.* 2005b). The origin of the affinity difference is not known, but the difference appears to arise from two separate forms of VAChT that do not affect binding of [^{3}H]vesamicol. Specific binding was fitted with biphasic competition eq. 1.

$$\text{Bound}=F_{HA}\left(1-\frac{\text{ACh}}{K_{AChHA}+\text{ACh}}\right)+(1-F_{HA})\left(1-\frac{\text{ACh}}{K_{AChLA}+\text{ACh}}\right) \quad (1)$$

F_{HA} is the fraction of high-affinity ACh binding, (1-F_{HA}) is the fraction of low-affinity ACh binding, ACh is the concentration of ACh (mM), and K_{AChHA} and K_{AChLA} are the equilibrium dissociation constants (mM) for the high- and low-affinity sites, respectively. Eq. 1 also was modified by fixing F_{HA} to 1 and K_{AChLA} to 10^6. This procedure creates a monophasic, single-affinity fit. Although the K_M value for transport is lower than the K_{AChHA} value for equilibrium binding, only K_{AChHA} is referred to as high-affinity, as transport of ACh always exhibits a single affinity.

Parameter values are given in Table 1 to two significant figures. Mutants exhibiting an abnormal parameter value were characterized several times, and values reported in Table 1 are from representative experiments. All measurements were done in groups of mutants that included wild-type VAChT as positive control. Quoted errors are ± one standard deviation. Except for F_{HA}, a parameter value must be greater than 3 propagated standard deviations and a factor of two different from that of wild-type to be considered abnormal (Ojeda *et al.* 2004). The factor-of-two requirement was not applied to F_{HA}, as the value of this parameter is bounded by 0 and 1. B_{max} values are used to compute the rate of transport normalized to the amount of expression (V_{max}/B_{max}). The regression results include calculation of a Model

Selection Criterion (based on the Akaike Information Criterion), which estimates goodness of fit adjusted for the number of degrees of freedom. The higher value for the Model Selection Criterion for monophasic and biphasic fits to ACh competition data determined the preferred fit to each data set.

Results and discussion

Site-directed mutagenesis and stable expression

Each clonal line for a mutant was characterized by western blot to determine if the VAChT expression level was adequate and minimal proteolysis and proper glycosylation occurred. The most highly expressing line was selected for preparative growth of each mutant. Also, cellular immunofluorescence arising from staining of VAChT and synaptophysin (a marker for synaptic-like microvesicles) was monitored for each mutant (Bonzelius *et al.* 1994). All mutants had western blot and immunofluorescence patterns similar to those of wild-type, indicating that no glycosylation, proteolysis, or intracellular trafficking problems occur due to the mutations.

Postnuclear supernatant was prepared and used to characterize (a) binding properties for [^{3}H] vesamicol, (b) equilibrium dissociation constants for ACh competing against subsaturating [^{3}H]vesamicol, and (c) transport properties for [^{3}H]ACh (Table 1). Under non-transporting conditions, VAChT has the conformation of the homology model (Nguyen *et al.* 1998). Thus, the model is directly relevant to interpretation of equilibrium experiments.

All mutants expressed well, as they exhibited B_{max} values for [^{3}H]vesamicol binding between 13 to 93 pmol/mg protein. This range compares with prior expression levels of about 10 pmol/mg protein that yielded reliable data (Varoqui and Erickson 1996; Kim *et al.* 1999; Zhu *et al.* 2001). The B_{max} values vary because the vector incorporates into the genome at random locations, some allowing more and some less expression. A few of the mutants yielded relatively low values of B_{max} for all clonal lines, possibly because the mRNA is unstable or the polypeptide is inserted into endoplasmic reticulum at low efficiency. B_{max} values correlated with staining intensity in western blots and are thought to be the same as pmol VAChT/mg protein. The equivalence is supported by the observation that the presence or absence of ATP and protonmotive force does not affect the value of B_{max} or K_v (Bravo *et al.* 2004a).

VAChT that expresses at a low level transports less [^{3}H]ACh simply because there is less of it. To account for this effect, transport rates are divided by the B_{max} value obtained from the same preparation of post-nuclear supernatant to calculate normalized transport rates and the normalized maximal transport rate (V_{max}/B_{max}). A mutation that affects transport rate should alter this number, which is similar to the turnover rate (or number of catalytic cycles per min) for an enzyme. The values of other parameters do not depend on expression levels and are not normalized for expression.

Another effect on transport could arise from overload of intracellular trafficking mechanisms when the expression level is high. The effects of aberrant trafficking on the functional properties of VAChT have been well studied in PC12 cells. VAChT normally traffics to synaptic-like microvesicles. Secondary destinations are large dense-core vesicles and early endosomes (Bauerfeind *et al.* 1993; Liu and Edwards 1997; Tao-Cheng and Eiden 1998; Varoqui and Erickson 1998a; Krantz *et al.* 2000; Ferreira *et al.* 2005). Both of the latter compartments generate robust protonmotive force and transport neurotransmitters well. The S480A mutation blocks phosphorylation of VAChT by protein kinase C and directs all VAChT away from synaptic-like microvesicles and into other membranes. Nevertheless, K_M, V_{max}, and K_v values for the S480A mutant are normal (Cho *et al.* 2000). Most of the mutants studied here that expressed at higher levels than wild type exhibit normal transport (namely **W325**F,

C388A, and **F392**A). Of the mutants studied here that exhibit decreased transport (namely Y60H, **F231**A, **W331**A, and A334F), only **F231**A expressed at a higher level than wild type, and that was by a modest amount. Even if mistargeting occurs because of over expression, there is an abundance of evidence that transport and binding parameters are not significantly altered by this event.

Because the project sought primarily to better define the locations of the ACh and vesamicol binding sites, we focus on equilibrium affinities. Normal values are ~10 mM for K_{AChHA} and ~20 nM for K_v. Only data documenting abnormal equilibrium affinity for ACh or vesamicol are shown, as graphs for these types of experiments have been published by this laboratory many times and normal behavior is of lesser interest. Mutations that perturb the fraction of high-affinity binding by ACh (F_{HA}) or the normalized maximal transport rate (V_{max}/B_{max}) are discussed briefly in the belief that their significance will be interpretable in the future. Abnormal values for parameters other than B_{max} are highlighted in Table 1 in boldface font.

Confirmation that mutations of W331 impair ACh but not vesamicol binding

W331 was mutated again in order to verify its importance in an ortholog of rVAChT, test the reproducibility of earlier results, and determine the effects of a new mutation in the residue (Table 1). **W331**A and **W331**L in hVAChT bind ACh 11- and 10-fold more weakly than wild-type does, respectively, and the ACh binding site in these mutants exhibits single affinity (Fig. 2A). The latter behavior might be an artifact born of weaker binding by the low-affinity site and our inability, due to experimental limitations, to observe very low-affinity binding. **W331**A exhibited no transport. As before, there is no effect on vesamicol affinity. Thus, properties of mutated W331 are reproducible in hVAChT (Ojeda *et al.* 2004).

Properties of new mutations near W331 in the homology model

Two groups of residues in the vicinity of **W331** and the closed region of the transport channel were chosen for mutation. The first group is composed of two residues lateral to **W331** and in the first bundle of TMs. The residues are (a) highly conserved but not invariant Y60 (the residue in snail is F) in the beginning of lumenal Loop I/II and (b) invariant **F231** in the lumenal end of TM V (Fig. 1). Y60 and **F231** each are ~10 Å away from **W331**. For comparison, the distance between the carbon nuclei in two pairs of C-H groups pointing directly toward each other with the H atoms in van der Waals contact is 4.0 Å (Lide 2010). Bound ACh would occupy a very significant fraction of the distance between Y60 or **F231** and **W331**, and mutations in these residues should have significant effects on ACh affinity, if ACh were bound in this region.

The only effect on equilibrium binding caused by these mutations is 2-fold *tighter* binding of ACh by Y60W (Fig. 2A; Table 1). Because Y60A, Y60H, and **F231**A do not affect binding of ACh, Y60 and **F231** are not part of the ACh binding site. The increased affinity by Y60W probably is caused by the larger residue causing a conformational change in a distant binding site for ACh. The mutants exhibit normal vesamicol binding. Thus, Y60 and **F231** are not part of the vesamicol binding site either. Overall, the results provide no support for an ACh or vesamicol binding site in the beginning of lumenal Loop I/II, lumenal end of TM V, or the closed region of the transport channel bounded by the triangle formed by Y60, **F231**, and **W331**.

However, Y60H and **F231**A decrease the transport rate (Table 1). This effect might occur because the mutations uncouple proton efflux from ACh transport or induce a large proton leak that destroys the protonmotive force (Parsons 2000). The phenolic hydroxyl group in Y60 plays no important role in transport, as Y60A and Y60W transport normally and snail VAChT has F in this position.

The second group chosen for mutation is composed of eleven residues within 8 Å of **W331** and in the second bundle of TMs (Fig. 1; Table 1). The residues are (a) **W315**, **M316**, and K317 in the lumenal end of TM VII, (b) **M320**, A321, **W325**, and A330 in lumenal Loop VII/VIII, (c) **W331** and highly conserved A334 (the residue in snail and *C. elegans* is S or P) in the lumenal beginning of TM VIII, and (d) highly conserved C388 (the residue in *Ciona*, snail, and *C. elegans* is A, M, or S), **C391**, and **F392** in the lumenal beginning of TM X. Residues 315–334 were investigated carefully because they include three invariant W residues that potentially could form a binding pocket. Most proteins that bind choline derivatives do so by solvating the quaternary ammonium group with aromatic side chains, the best of which is W (Zacharias and Dougherty 2002). Residues in the regions of TMs IX, XI, and XII lateral to **W331** were not mutated because they are located well away from the transport channel and unlikely to be accessible to ACh coming from cytoplasm.

In the second group of residues, only A330V and A334F in the lumenal beginning of TM VIII have effects on equilibrium binding (Table 1). A330V exhibits a 2-fold decrease in the fraction of high-affinity binding by ACh without effect on ACh or vesamicol affinity. Because the origin of high- and low-affinities is not known, a mechanistic interpretation of the effect is not possible. Regardless, the lack of effect on affinities *per se* indicates that A330 is not at the ACh or vesamicol binding site. In contrast, A334F binds ACh 14-fold and vesamicol 4-fold less tightly than wild-type does (Fig. 2A and 2B). This mutant also exhibits apparent monophasic binding of ACh.

Two of the mutants in the second group exhibit abnormal transport. A334F transports about one-half as fast as wild-type does. On the other hand, **C391**A transports about 2-times faster than wild-type does. Molecular interpretation of these effects currently is not possible.

Prior mutations near W331 in the homology model

Other published information is consistent and no published information is inconsistent with the results obtained here. Ojeda *et al.* (2004) found that **F335**A exhibits ~3-fold weaker binding of vesamicol. Zhu *et al.* (2001) found that **C391**Y does not bind vesamicol. It also exhibits 2.6-fold higher K_M value for transport, which indicates it might bind ACh somewhat weaker than wild type does. The speculation cannot be proved, however, as without binding of [^{3}H] vesamicol, equilibrium binding of ACh cannot be measured. **C391**Y and **W331**/A/F/L strongly resolve the binding sites for ACh and vesamicol from each other.

H63A, **A228**G, **A228**V, G233A, G233F, and H318A also have been characterized (Kim *et al.* 2000; Zhu *et al.* 2001; Ojeda *et al.* 2004; Chandrasekaran *et al.* 2006). The results demonstrate that vesamicol and ACh binding are not associated with the lumenal end of TM V or lumenal loops I/II, V/VI, and VII/VIII. Varoqui and Erickson (1998b) constructed a chimera replacing the first 129 residues of hVAChT with the corresponding sequence from closely related human vesicular monoamine transporter 2. The results demonstrate that vesamicol binding is not associated with the N-terminal domain or loop I/II.

Mutations near the lumenal mouth that decrease equilibrium affinity form a cluster

A total of 21 residues in and near **W331** and the lumenal mouth of the transport channel have been mutated by all researchers (Fig. 1). Mutations in **W331**, highly conserved A334, and **F335** in TM VIII and **C391** in TM X decrease equilibrium affinity for ACh and/or vesamicol. Mutations in 17 other residues near **W331** do not, thus excluding these residues as part of the ACh or vesamicol binding site. A334 and **F335** are a little less or more than one helical turn after **W331** in the lumenal beginning of TM VIII (this TM runs toward cytoplasm). **W331**, A334, and **F335** point approximately in the same direction from the helical axis of TM VIII toward TM X, which lies alongside of TM X (Fig. 3). In reciprocal manner, **C391** in TM X

points toward **W331** in TM VIII. Mutations deleterious to equilibrium binding of ACh and/or vesamicol in or close to the lumenal region of the transport channel form a cluster.

How are clustered lumenal residues important to ACh and vesamicol binding?

The simplest hypothesis for the function of the **W331**, highly conserved A334, **F335**, and **C391** cluster retains the rocker-switch model for transport with the variation that the single binding site for ACh is extraordinarily deep in the transport channel, as described in the introduction. However, VAChT binds and transports many monovalent organic cations in addition to ACh, such as ethidium and tetraphenylphosphonium (Bahr *et al.* 1992; Clarkson *et al.* 1992; Bravo *et al.* 2004b, 2005a). The structural range of substrates is so wide that it is improbable a single binding site can accommodate all of them. It is likely each type of VAChT substrate binds to a different site, as occurs in multidrug resistance transporters (Fluman and Bibi 2009). The transport channel in the VAChT homology model has a large surface area and many pockets and cavities that might serve as binding sites (Dundas *et al.* 2006). It would be of interest to test the effects of mutations that impair affinity for ACh on affinities for other substrates.

The possible presence of multiple binding sites for substrates suggests an additional transport model for ACh. There might be two (or more) separate sites for ACh. Separate binding sites probably would require the transport pathway to resemble a classical channel. Computer-based simulations of transport by GlpT suggest that a channel-like transport pathway might exist when the tilt angle between TM bundles is small (Tsigelny *et al.* 2008). The simulations are relevant, as GlpT is the template for the three-dimensional model of VAChT. They suggest that an important difference between single-site and multi-site models for substrate binding could be as little as whether the TM bundles exhibit large- or small-amplitude fluctuation in the tilt angle between them. A transport pathway resembling a classical channel containing two separate binding sites for glucose has much experimental support in the MFS protein GLUT1 (Carruthers *et al.* 2009).

The topological location of the cluster investigated here somewhat resembles that for one of the clusters of residues important to substrate recognition by MdfA, which is a multidrug transporter in *E. coli* (Adler and Bibi 2004). One MdfA cluster is close to cytoplasm, and the other one is close to periplasm (which corresponds to the lumen of synaptic vesicles). Drug is hypothesized to interact sequentially with each cluster as it passes through the transport pathway, somewhat like transport by GLUT1. However, the TMs contributing to the periplasmic cluster in MdfA are different from those contributing to the lumenal cluster in VAChT, and no cluster of residues important to binding of ACh or vesamicol near cytoplasm is known for VAChT.

Many mutations in VAChT residues **D398**, **K131**, and **D425** inhibit transport of [^{3}H]ACh and binding of [^{3}H]vesamicol (Kim *et al.* 1999, 2000; Bravo *et al.* 2005b). These residues are located approximately midway along the transport pathway. However, they probably are not in the ACh or vesamicol binding site *per se*. **D398**E transports [^{3}H]ACh well, which means it must bind ACh well despite the mutation. The “reversed” double-mutant **H338**D/**D398**H binds [^{3}H]vesamicol well, which suggests that interaction between **H338** and **D398** controls the conformation of a separate binding site for vesamicol. Mutants **K131**A, **K131**H, **D425**N, and **D425**H bind ACh and vesamicol with normal or even greater than normal affinities, also suggesting that **K131** and **D425** control the conformations of separate sites for ACh and vesamicol.

A mechanistic model for VAChT that has two binding sites for ACh in fact has been proposed (Varoqui and Erickson 1997). One site is close to cytoplasm, the other site is close to vesicular lumen, and transfer of bound ACh between them occurs during transport, similarly to proposals

for MdfA and GLUT1. This model makes a paradoxical prediction. A nonconservative mutation that destroys one of the binding sites might not decrease equilibrium molecular affinity of VAChT for ACh, as the non-mutated site could remain intact. However, the mutation presumably would block transport, as sequential binding to each site is required. Because ACh binding could appear normal (although it isn't), loss of transport could be misinterpreted as blockade of a post-binding step like proton binding. Other confusing phenotypes also are possible. Could the two-site model of Varoqui and Erickson (1997) explain high- and low-affinity binding of ACh at equilibrium? Possibly, but a specific model satisfying all data has not been devised.

Diverse mutational and computational results are raising the possibility that the rocker-switch model with its single binding site for substrate located midway through the transport channel does not apply to all members of the MFS. Current evidence for VAChT is consistent with a single binding site for ACh in the vicinity of **W331**, highly conserved A334, **F335**, and **C391** very low in the transport pathway. The site probably would be destroyed by rocker switch, were it to occur, but there is no information on this speculation. However, despite a paucity of data supporting the existence of a second, topologically distinct binding site for ACh, the single-site hypothesis is not strong, as other regions of VAChT have not been comprehensively probed. Also, as discussed above, two-site binding by ACh could deceive. More evidence is required about the nature of the ACh binding site(s).

The vesamicol binding site has fundamentally different properties from the ACh binding site (s). It is fastidious, as only vesamicol and its close analogues bind with high affinity, and only monophasic binding ever has been observed (Rogers *et al.* 1989). This behavior implies that strong, specific contacts between vesamicol and a single, substantially preformed binding site are made. However, here too further information is required to locate the site. But if VAChT is substrate-promiscuous, why isn't vesamicol a substrate? The answer probably is that vesamicol binds so tightly that its dissociation rate is too slow for a transported molecule (Rogers *et al*. 1993). Moreover, even if vesamicol were transported slowly, as a tertiary amine it would leak out of the vesicle and not accumulate.

Acknowledgments

This research was supported by grant NS15047 from the National Institute of Neurological Disorders and Stroke. We thank Eyal Vardy and Shimon Schuldiner for providing coordinates of the VAChT homology model.

References

Abramson J, Iwata S, Kaback HR. Lactose permease as a paradigm for membrane transport proteins. Mol Membr Biol 2004;21:227–236. [PubMed: 15371012]

Adler J, Bibi E. Determinants of substrate recognition by the *Escherichia coli* multidrug transporter MdfA identified on both sides of the membrane. J Biol Chem 2004;279:8957–8965. [PubMed: 14688269]

Bahr BA, Clarkson ED, Rogers GA, Noremberg K, Parsons SM. A kinetic and allosteric model for the acetylcholine transporter-vesamicol receptor in synaptic vesicles. Biochemistry 1992;31:5752–5762. [PubMed: 1319200]

Bauerfeind R, Regnier-Vigouroux A, Flatmark T, Huttner WB. Selective storage of acetylcholine, but not catecholamines, in neuroendocrine synaptic-like microvesicles of early endosomal origin. Neuron 1993;11:105–121. [PubMed: 8338662]

Bonzelius F, Herman G, Cardone M, Mostov K, Kelly R. The polymeric immunoglobulin receptor accumulates in specialized endosomes but not synaptic vesicles within the neurites of transfected neuroendocrine PC12 cells. J Cell Biol 1994;127:1603–1616. [PubMed: 7798315]

Bravo DT, Kolmakova NG, Parsons SM. Transmembrane reorientation of the substrate-binding site in vesicular acetylcholine transporter. Biochemistry 2004a;43:8787–8793. [PubMed: 15236587]

Bravo DT, Kolmakova NG, Parsons SM. Choline is transported by vesicular acetylcholine transporter. J Neurochem 2004b;91:766–768. [PubMed: 15485505]

Bravo DT, Kolmakova NG, Parsons SM. New transport assay demonstrates vesicular acetylcholine transporter has many alternative substrates. Neurochem Intern 2005a;47:243–247.

Bravo DT, Kolmakova NG, Parsons SM. Mutational and pH analysis of ionic residues in transmembrane domains of vesicular acetylcholine transporter. Biochemistry 2005b;44:7955–7966. [PubMed: 15924414]

Carruthers A, De Zutter J, Ganguly A, Devaskar SU. Will the original glucose transporter isoform please stand up! Am J Physiol 2009;297:E836–E848.

Chandrasekaran A, Ojeda AM, Kolmakova NG, Parsons SM. Mutational and bioinformatics analysis of proline- and glycine-rich motifs in vesicular acetylcholine transporter. J Neurochem 2006;98:1551–1559. [PubMed: 16923166]

Cho GW, Kim MH, Chai YG, Gilmor ML, Levey AI, Hersh LB. Phosphorylation of the rat vesicular acetylcholine transporter. J Biol Chem 2000;275:19942–19948. [PubMed: 10748073]

Clarkson ED, Rogers GA, Parsons SM. Binding and active transport of large analogs of acetylcholine by cholinergic synaptic vesicles *in vitro*. J Neurochem 1992;59:695–700. [PubMed: 1629738]

Dastmalchi S, Beheshti S, Morris MB, Church WB. Prediction of rotational orientation of transmembrane helical segments of integral membrane proteins using new environment-based propensities for amino acids derived from structural analyses. FEBS J 2007;274:2653–2660. [PubMed: 17451441]

DeLano, WL. The PyMOL Molecular Graphics System. DeLano Scientific; Palo Alto, CA, USA: 2002. Available at: http://www.pymol.org

Dundas J, Ouyang Z, Tseng J, Binkowski A, Turpaz Y, Liang J. CASTp: computed atlas of surface topography of proteins with structural and topographical mapping of functionally annotated residues. Nucleic Acids Res 2006;34:W116–W118. [PubMed: 16844972]

Eudes A, Kunji ERS, Noiriel A, Klaus SMJ, Vickers TJ, Beverley SM, Gregory JF III, Hanson AD. Identification of transport-critical residues in a folate transporter from the folate-biopterin transporter (FBT) family. J Biol Chem 2010;285:2867–2875. [PubMed: 19923217]

Ferreira LT, Santos MS, Kolmakova NG, Koenen J, Barbosa J Jr, Gomez MV, Guatimosim C, Zhang X, Parsons SM, Prado VF, Prado MAM. Structural requirements for steady-state localization of the vesicular acetylcholine transporter. J Neurochem 2005;94:957–969. [PubMed: 16092939]

Fluman N, Bibi E. Bacterial multidrug transport through the lens of the major facilitator superfamily. BBA-Proteins Proteom 2009;1794:738–747.

Jeon, J.; Yang, J-S.; Kim, S. Integration of evolutionary features for the identification of functionally important residues in major facilitator superfamily transporters. PLoS Comput Biol. 2009. No pp. given. Available at http://www.ploscompbiol.org/article/fetchObjectAttachment.action?uri=info%3Adoi%2F10.1371%2Fjournal.pcbi.1000522&representation=PDF

Khare P, White AR, Parsons SM. Multiple protonation states of vesicular acetylcholine transporter detected by binding of [^{3}H]vesamicol. Biochemistry 2009;48:8965–8975. [PubMed: 19685929]

Kim MH, Lu M, Lim EJ, Chai YG, Hersh LB. Mutational analysis of aspartate residues in the transmembrane regions and cytoplasmic loops of rat vesicular acetylcholine transporter. J Biol Chem 1999;274:673–680. [PubMed: 9873001]

Kim MH, Lu M, Kelly M, Hersh LB. Mutational analysis of basic residues in the rat vesicular acetylcholine transporter. Identification of a transmembrane ion pair and evidence that histidine is not involved in proton translocation. J Biol Chem 2000;275:6175–6180. [PubMed: 10692409]

Krantz DE, Waites C, Oorschot V, Liu Y, Wilson RI, Tan PK, Klumperman J, Edwards RH. A phosphorylation site regulates sorting of the vesicular acetylcholine transporter to dense core vesicles. J Cell Biol 2000;149:379–395. [PubMed: 10769030]

Law CJ, Almqvist J, Bernstein A, Goetz RM, Huang Y, Soudant C, Laaksonen A, Hovmoeller S, Wang DN. Salt-bridge dynamics control substrate-induced conformational change in the membrane transporter GlpT. J Mol Biol 2008a;378:826–837.

Law CJ, Maloney PC, Wang DN. Ins and outs of major facilitator superfamily antiporters. Ann Rev Microbiol 2008b;62:289–305. [PubMed: 18537473]

Law CJ, Enkavi G, Wang DN, Tajkhorshid E. Structural basis of substrate selectivity in the glycerol-3-phosphate: phosphate antiporter GlpT. Biophys J 2009;97:1346–1353. [PubMed: 19720022]

Lide, DR., editor. CRC Handbook of Chemistry and Physics, 90th Edition (Internet Version 2010). CRC Press/Taylor and Francis; Boca Raton, FL: 2010. Atomic Radii of the Elements; p. 9-49.

Liu Y, Edwards RH. Differential localization of vesicular acetylcholine and monoamine transporters in PC12 cells but not CHO cells. J Cell Biol 1997;139:907–916. [PubMed: 9362509]

Nguyen ML, Cox GD, Parsons SM. Kinetic parameters for the vesicular acetylcholine transporter: Two protons are exchanged for one acetylcholine. Biochemistry 1998;37:13400–13410. [PubMed: 9748347]

Ojeda AM, Kolmakova NG, Parsons SM. Acetylcholine binding site in the vesicular acetylcholine transporter. Biochemistry 2004;43:11163–11174. [PubMed: 15366926]

Parsons SM. Transport mechanisms in acetylcholine and monoamine storage. FASEB J 2000;14:2423–2434. [PubMed: 11099460]

Patching SG, Psakis G, Baldwin SA, Baldwin J, Henderson PJF, Middleton DA. Relative substrate affinities of wild-type and mutant forms of the *Escherichia coli* sugar transporter GalP determined by solid-state NMR. Mol Membr Biol 2008;25:474–484. [PubMed: 18798051]

Rogers GA, Parsons SM. Inhibition of acetylcholine storage by acetylcholine analogs *in vitro*. Mol Pharmacol 1989;36:333–341. [PubMed: 2770706]

Rogers GA, Parsons SM, Anderson DC, Nilsson LM, Bahr BA, Kornreich WD, Kaufman R, Jacobs RS, Kirtman B. Synthesis, *in vitro* acetylcholine-storage-blocking activities, and biological properties of derivatives and analogs of *trans*-2-(4-phenylpiperidino)cyclohexanol (vesamicol). J Med Chem 1989;32:1217–1230. [PubMed: 2724295]

Rogers GA, Kornreich WD, Hand K, Parsons SM. Kinetic and equilibrium characterization of vesamicol receptor-ligand complexes with picomolar dissociation constants. Mol Pharmacol 1993;44:633–641. [PubMed: 8371715]

Saier MHJ, Beatty JT, Goffeau A, Harley KT, Heijne WH, Huang SC, Jack DL, Jahn PS, Lew K, Liu J, Pao SS, Paulsen IT, Tseng TT, Virk PS. The major facilitator superfamily. J Mol Microbiol Biotechnol 1999;1:257–279. [PubMed: 10943556]

Tao-Cheng JH, Eiden LE. The vesicular monoamine transporter VMAT2 and vesicular acetylcholine transporter VAChT are sorted to separate vesicle populations in PC12 cells. Adv Pharmacol 1998;42 (Catecholamines):250–253. [PubMed: 9327891]

Tsigelny IF, Greenberg J, Kouznetsova V, Nigam SK. Modeling of glycerol-3-phosphate transporter suggests a potential 'tilt' mechanism involved in its function. J Bioinf Comp Biol 2008;6:885–904.

Tu Z, Efange SMN, Xu J, Li S, Jones LA, Parsons SM, Mach RH. Synthesis and *in vitro* and *in vivo* evaluation of ^{18}F-labeled positron emission tomography (PET) ligands for imaging the vesicular acetylcholine transporter. J Med Chem 2009;52:1358–1369. [PubMed: 19203271]

Vardy E, Arkin IT, Gottschalk KE, Kaback HR, Schuldiner S. Structural conservation in the major facilitator superfamily as revealed by comparative modeling. Protein Sci 2004;13:1832–1840. [PubMed: 15215526]

Varoqui H, Erickson JD. Active transport of acetylcholine by the human vesicular acetylcholine transporter. J Biol Chem 1996;271:27229–27232. [PubMed: 8910293]

Varoqui H, Erickson JD. Vesicular neurotransmitter transporters. Potential sites for the regulation of synaptic function. Mol Neurobiol 1997;15:165–192. [PubMed: 9396009]

Varoqui H, Erickson JD. The cytoplasmic tail of the vesicular acetylcholine transporter contains a synaptic vesicle targeting signal. J Biol Chem 1998a;273:9094–9098. [PubMed: 9535898]

Varoqui H, Erickson JD. Dissociation of the vesicular acetylcholine transporter domains important for high-affinity transport recognition, binding of vesamicol and targeting to synaptic vesicles. J Physiology-Paris 1998b;92:141–144.

Volknandt W, Zimmermann H. Cholinergic synaptic vesicles isolated from motor nerve terminals from electric fishes to rat. Molecular composition and functional properties. Ann NY Acad Sci 1987;493Cell Mol Biol Horm-Neurotransm-Containing Secretory Vesicles :159–161.

Yang Q, Wang X, Ye L, Mentrikoski M, Mohammadi E, Kim YM, Maloney PC. Experimental tests of a homology model for OxlT, the oxalate transporter of *Oxalobacter formigenes*. P Natl Acad Sci USA 2005;102:8513–8518.

Zacharias N, Dougherty DA. Cation-π interactions in ligand recognition and catalysis. Trends Pharmacol Sci 2002;23:281–287. [PubMed: 12084634]

Zhu H, Duerr JS, Varoqui H, McManus JR, Rand JB, Erickson JD. Analysis of point mutants in the *Caenorhabditis elegans* vesicular acetylcholine transporter reveals domains involved in substrate translocation. J Biol Chem 2001;276:41580–41587. [PubMed: 11551909]

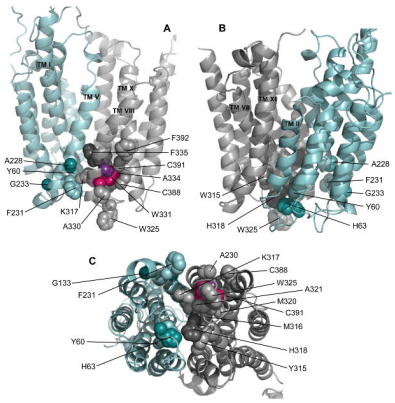

Fig. 1.

Homology model of hVAChT showing mutated residues. Non-TM regions are clipped off. The first bundle of TMs is teal and the second bundle is gray. Cytoplasm is at the top in Views A and B. Odd-numbered TMs run toward vesicular lumen, and even-numbered TMs run toward cytoplasm. The side chains and C_αs of mutated residues are shown as van der Waals spheres and labeled with the position numbers. A residue mutated in this study is the color of the host bundle of TMs, and the properties of the mutant are listed in Table 1. A residue mutated in other studies is a darker shade of the color of the host bundle, and the properties of the mutant are discussed in the text. Exceptions to this color scheme are **W331** in magenta and A334 in purple in the beginning of TM VIII. **View A**. Side of VAChT seen from within the bilayer. **View B**. View A was rotated ~180° around the transport axis. **View C**. An observer inside vesicular lumen would see this view. Figures were rendered using PyMOL (DeLano 2002).

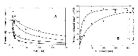

Fig. 2.

Abnormal equilibrium binding to mutants. Frame A. Displacement of 5 nM [^{3}H]vesamicol by the indicated concentration of ACh. Wild-type (▲), Y60W (■), **W331**L (*), and A334F (●) are shown. Wild type and most mutants exhibit high-affinity (K_{AChHA}, displacement mostly below 40 mM ACh) and low-affinity (K_{AChLA}, displacement mostly above 100 mM ACh) components. Frame B. [^{3}H]vesamicol binding. The indicated concentrations of [^{3}H]vesamicol were equilibrated with wild type (▲) or A334F (■). Parameters for all mutants are listed in Table 1.

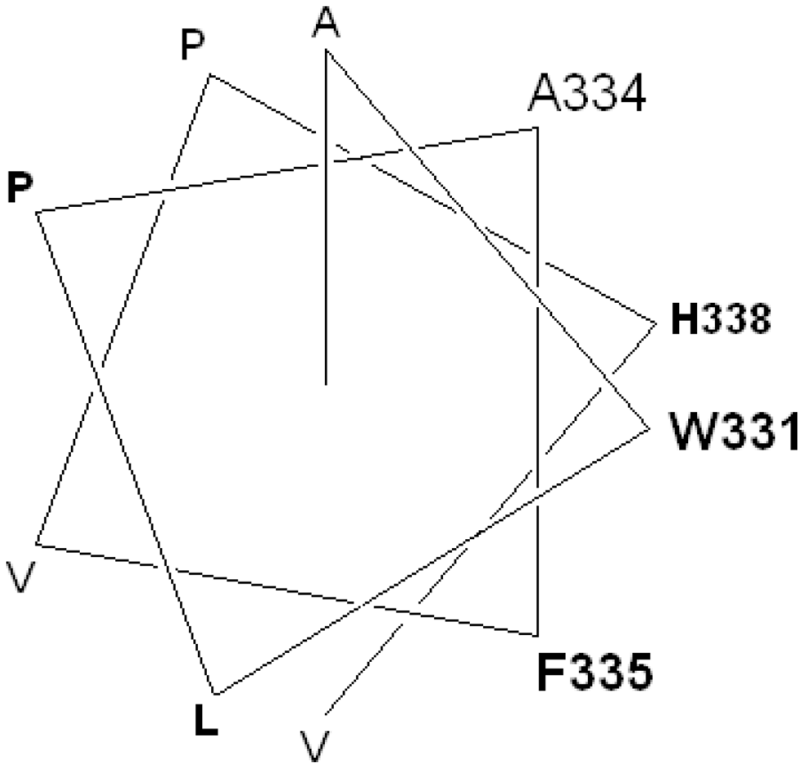

Fig. 3.

Helical-wheel view of the lumenal beginning of TM VIII. The sequence is A**W**^{331}**LP**A^{334}**F**^{335}VP**H**^{338}V, where bold face indicates an invariant residue. The numbered residues are special. The vertical line indicates the beginning of the wheel, which recedes away from an observer who is inside of the synaptic vesicle. In the homology model, TM X lies to the right. Drawn with the Helical TransMembrane Segment Rotational Angle Prediction program (Dastmalchi *et al.* 2007).

Table 1

Binding and transport by mutants in and around W331[a]

WT or Mutant[b]	TM or Loop	Å to W331[c]	K_v (nM)[d]	B_{max} (pmol/ mg)[e]	K_{AChHA}, K_{AChLA} (mM)[f]	F_{HA}[g]	K_M (mM)[h]	V_{max}/B_{max} (min^{-1})[i]
WT	-	-	22 ± 2	50 ± 1	11 ± 1, id[j]	0.82 ± 0.04	0.95 ± 0.20	6.8 ± 0.5
First bundle of TMs								
Y60A	I/II	10	25 ± 5	31 ± 2	8.2 ± 0.7, id[j]	0.92 ± 0.02	0.48± 0.32	4.7 ± 0.8
Y60H	I/II	10	14 ± 2	15 ± 1	11 ± 0, 4500 ± 100	0.82 ± 0.04	0.72 ± 0.53	**3.1 ± 0.6**
Y60W	I/II	10	26 ± 8	34 ± 3	**4.5 ± 0.1**, 92 ± 12	0.86 ± 0.02	0.92 ± 0.17	7.9 ± 0.8
F231A	V	7	24 ± 6	64 ± 4	5.8 ± 1.2, id[j]	0.67 ± 0.05	id[j]	**1.5 ± 1.3**[j]
Second bundle of TMs								
W315A	VII	6	11 ± 1	26 ± 1	11 ± 4, id[j]	0.84 ± 0.16	0.69 ± 0.22	5.2 ± 0.8
M316A	VII	3	29 ± 6	38 ± 2	8.3 ± 0.7, 160 ± 10	0.74 ± 0.03	1.5 ± 0.3	8.2 ± 1.0
K317A	VII	3	32 ± 6	21 ± 1	6.9 ± 1.2, 450 ± 330[j]	0.72 ± 0.06	3.2 ± 1.2	17.8 ± 3.9
M320A	VII/VIII	3	25 ± 3	62 ± 5	9.2 ± 0.8, 200 ± 140[j]	0.73 ± 0.11	id[j]	id[j]
A321F	VII/VIII	7	23 ± 3	21 ± 1	15 ± 2, 19,000 ± 10,000[j]	0.90 ± 0.06	0.35 ± 0.10	6.0 ± 0.5
W325H	VII/VIII	8	23 ± 4	22 ± 1	5.5 ± 0.9, 350 ± 300[j]	0.82± 0.06	0.48 ± 0.17	6.5 ± 1.1
W325F	VII/VIII	8	19 ± 3	75 ± 3	7.3 ± 1.6, 160 ± 70	0.74 ± 0.09	1.0 ± 0.3	5.0 ± 0.5
A330V	VII/VIII	5[k]	19 ± 1	21 ± 0	12 ± 5, 130 ± 30	**0.44 ± 0.11**	2.2 ± 0.9	6.3 ± 1.3
W331A	VIII	-	47 ± 6	37 ± 2	**120 ± 0**	**1.0**	**nt**[l]	**nt**[l]
W331L	VIII	-	33 ± 5	14 ± 1	**110 ± 10**	**1.0**	4.6 ± 1.5	6.2 ± 1.2
A334F	VIII	4	**92 ± 14**	13 ± 1	**150 ± 30**	**1.0**	3.0 ± 1.3	**3.6 ± 0.8**
C388A	X	6	26 ± 2	59 ± 1	17 ± 4, id[j]	0.88 ± 0.08	2.3 ± 0.5	12 ± 1
C391A	X	4	25 ± 8	34 ± 3	10 ± 3, 190 ± 150[j]	0.71 ± 0.07	1.8 ± 0.3	**15 ± 2**
F392A	X	8	31 ± 6	93 ± 5	7.9 ± 1.3, id[j]	0.91 ± 0.06	0.52 ± 0.11	11 ± 1

[a] At pH 7.4.

[b] Invariant residues are boldface.

[c] Shortest distance between the nucleus of any heavy atom (C, N, O, S) in the wild-type residue and the nucleus of any heavy atom in **W331**, rounded to 1 Å.

[d] Vesamicol dissociation constant.

[e] VAChT expression level.

[f] Dissociation constants for high-affinity and low-affinity binding of ACh. If only one number is given, only one affinity for ACh is exhibited.

[g] Fraction of the ACh sites that have high affinity.

[h] Michaelis-Menten constant for ACh transport.

[i] V_{max} for Michaelis-Menten transport normalized to B_{max} for the same postnuclear preparation.

[j] Indeterminate because the regression error was too large.

[k] Side-chain distance only.

[l] No transport.